47th AIAA/ASME/SAE/ASEE Joint Propulsion Conference & Exhibit
31 July - 03 August 2011, San Diego, California

AIAA 2011-6064

Examination of the Various Cycles for Pulse Detonation Engines

R. Vutthivithayarak,* Eric M. Braun† and Frank K. Lu‡
University of Texas at Arlington, Arlington, Texas 76019

An examination of three common thermodynamic cycles developed for detonation-based engine analysis, namely the Humphrey, Fickett–Jacobs and Zel'dovich–von Neumann–Döring, shows that the last one is the most appropriate in capturing the essential physics in a one-dimensional framework. It is suggested that a local thermodynamic equilibrium assumption be invoked for the shock and heat release processes. An engineering approach to constructing the ZND cycle and the need for precompression are addressed.

I. Introduction

AIRBREATHING pulse detonation engines (PDEs) have been developed because they have the potential to yield better performance than existing deflagration-based engines in terms of improved thermodynamic efficiency, simplicity of manufacture and operation, compactness and weight, amongst others. As is the case with all other heat engines, the theoretical performance of PDEs using thermodynamic cycle analysis requires an accurate thermodynamic model. The focus of this paper is to evaluate different models that have been applied to PDEs. The study is limited in scope to ideal thermodynamic cycles and it does not consider in detail various elements that form an actual propulsion system.

Thermodynamic cycle analysis of heat engines is a standard technique for understanding the relationship between energy, heat and work involving simple compressible substances. Thermodynamic cycle analysis requires that the state of the system changes under the assumption of a quasi-static or equilibrium process.[1] Such a process is sufficiently slow for the system to be close to the equilibrium state so that all properties within the system are uniform. Another assumption is that gradients are infinitesimally small. Moreover, these assumptions are applied to cycles involving combustion with disregard to further complications involving chemical nonequilibrium. For most thermodynamic processes of engineering interest, the equilibrium and uniformity assumptions are sufficient, at least in terms of serving as idealizations of actual processes. In particular, the Brayton cycle is used to idealize a gas turbine engine where a working fluid is isentropically compressed, isobarically heated, isentropically expanded and then isobarically cooled in a closed cycle. In fact, the isobaric heating process is due to the combustion of the working fluid, in this case, air, with a fuel, a nonequilibrium process. In summary, the actual processes in a heat engine are idealized to allow engineering analysis to proceed.

Turning to a different type of engine that utilizes shocks or detonation waves, perhaps the first practical implementation of cycle analysis for an engine with non-isobaric heat addition was by Humphrey.[2] This analysis approach paved the way for considering engines with shocks or detonation waves. Prior to this

*Graduate Research Associate, Aerodynamics Research Center, Department of Mechanical and Aerospace Engineering.
†Graduate Research Associate, Aerodynamics Research Center, Department of Mechanical and Aerospace Engineering. Student Member AIAA.
‡Professor and Director, Aerodynamics Research Center, Department of Mechanical and Aerospace Engineering. Associate Fellow AIAA.

invention, development of the Chapman–Jouguet (CJ) theory for one-dimensional propagation of detonation waves occurred.[3,4] In the CJ theory, chemical reactions are modeled as a heat release in an infinitesimally thin, shock front that brings the material from an initial state on the inert Hugoniot to the subsequent state, known as the CJ point, on the reactive Hugoniot.[5,6] The CJ point is also the tangent from the initial state to the final state on a p–v diagram. This tangent line can be shown to be equal to the Rayleigh heating process.

Despite the occurrence of a detonation in Humphrey's engine, the process is strictly a constant volume one. Thus, Humphrey did not apply the CJ theory but developed a cycle based on constant volume heat addition, followed by an isentropic expansion and an isobaric heat rejection. This basic, three-step process is now known as the *Humphrey cycle*. Some authors add an additional, isentropic precompression process.[a]

Subsequent to the CJ theory, Zel'dovich, von Neumann and Döring independently developed a more elaborate one-dimensional theory now known as the Zel'dovich–von Neumann–Döring (ZND) theory.[7–9] In this theory, the propagating detonation wave consists of a shock that raises the initial state to an intermediate, von Neumann state, also known as the ZND point, which triggers the chemical reactions. Unlike the CJ theory where the heat release occurs instantly, the ZND theory allows the heat release to occur from the ZND to the CJ point. The ZND→CJ path is the straight line tangent to the CJ point and can be viewed as supersonic heat addition that drives the flow to the sonic, CJ point. This straight line, upon extrapolation, reaches the initial state.

Cycle analysis of PDEs has been performed, for example, in Refs. [10]–17] to name a few. Cycle analysis in detonation systems poses a number of difficulties associated with the unsteady flow. The first and simplest approach is to ignore the high-speed flow due to the shock and utilize the Humphrey cycle.[11–13,15,16] As remarked by Heiser and Pratt,[10] the Humphrey cycle while used as a surrogate for the actual PDE cycle produces a value of the thermal efficiency which is close to but less than that of an ideal PDE cycle.

Two other cycles have also been used. These utilize either the CJ or the ZND models, although sophisticated techniques involving numerical modeling have also been developed.[14] The so-called *Fickett–Jacobs* cycle relies on the CJ model for the detonation.[18] In this cycle, the CJ point is approached via a Rayleigh heat addition process, that is, along the tangent in the p–v diagram. The working gas is then expanded isentropically to the initial pressure and the cycle is closed by isobaric heat rejection.

A number of authors, however, consider that the most appropriate cycle is based on the ZND model.[10] This model is known as the *ZND cycle* in the current. In the ZND cycle, the working gas is compressed to the ZND point along the shock hugoniot. While it is understood that the shock process is a nonequilibrium one, the consensus is that this process can be represented along the inert hugoniot, invoking the local thermodynamic equilibrium (LTE) assumption. As applied here, LTE implies that the system is close to equilibrium and requires that the thermodynamic state evolves incrementally. Arguments for and against such an assumption abound which even question the basis of equilibrium thermodynamics.[19,20] It suffices to say that the LTE assumption for shock compression is consistent with other assumptions in ideal thermodynamic cycle analysis.

Next, Rayleigh heat release brings the gas from the ZND point to the CJ point. Subsequently, depending on the upstream boundary conditions, the gas generally undergoes an isentropic expansion, known as the Taylor expansion. The theoretical cycle closes when the gas returns to its initial state via isobaric heat rejection. Experimental observations indicate that the detonation front is actually a complex, three-dimensional surface that defies any simplified analytical description. Thus, despite the one-dimensional nature of the ZND model, it is presently acceptable for engineering analysis.

A. The Shock Compression Process for PDE Applications

Without attempting an esoteric discussion of nonequilibrium thermodynamics, consider instead an engineering approach limiting consideration to conditions expected in detonation-based engines. Consider a shock

[a]Note the similarity between the Humphrey cycle and the Otto cycle which is used to model the four-stroke internal combustion engine.

Table 1. Downstream conditions assuming equilibrium or frozen flow.

Gas	p (bar)		T (K)		h (kJ/kg)	
	Equilibrium	Frozen	Equilibrium	Frozen	Equilibrium	Frozen
Air	27.9	27.9	1510	1513	1349	1349
$O_2 + N_2$	28	27.9	1506	1507	1358	1358
$He + O_2 + N_2$	28.2	28.1	1600	1604	1625	1625
$Ar + O_2 + N_2$	28.2	28.1	1600	1604	1295	1295
$H_2 + O_2 + N_2$	15.8	27.8	2946	1531	1355	1874

wave propagating through a nonreactive mixture and a reactive mixture at an incident Mach number of 4.82 which corresponds to a speed of 1600–1800 m/s depending on the gas. This Mach number is typical of those due to propagating detonation waves and, in fact, is that of a stoichiometric hydrogen–air mixture. Data obtained from the NASA Chemical Equilibrium Application (CEA) code[21] for the downstream state with the gases initially at STP are displayed in Table 1. The first four rows for nonreactive gas mixtures show that the downstream states for either the equilibrium or frozen assumption are practically the same. It is next surmised that the approach to the final state occurs via LTE, that is, the path is along the inert hugoniot. This surmise has some support through consideration of the reactive mixture. The mixture first attains a state dictated by the ZND theory which is along the inert hugoniot. This step is similar to that of the nonreactive mixtures and yields the frozen condition. Next, the reactive mixture attains equilibrium through heat release.

II. The Cycles

While cycle analysis typically considers a generic working fluid, a specific reactant mixture and initial conditions are used here to facilitate the comparison. Consider a stoichiometric air and oxygen mixture initially at STP. Equilbrium conditions are obtained from the NASA CEA code[21] while nonequilibrium chemistry is obtained via Cantera.[22] Figure 1 shows the three ideal processes under discussion in both the p–v and T–s diagrams, portraying the total (or stagnation) states. The initial state of the reactants is (1). The hugoniot running through (1) is shown in Fig. 1(a) as a dashed line. The post-detonation hugoniot is also shown in the figure by another dashed line. This hugoniot was obtained using data obtained from the NASA CEA code,[21] yielding a dimensionless heat release $\alpha = q\rho_1/p_1 = 27.28$.

A. The Humphrey Cycle

As shown in Fig. 1, the gas, initially at (1) is compressed isochorically to state (2H) where $p_{2H} = 0.8$ MPa and $T_{2H} = 2550$ K. The gas then expands isentropically to reach (3H) where $p_{3H} = 0.1$ MPa and $T_{3H} = 1520$ K. The increase in entropy from (1) to (3H) is $\Delta s = 3.08$ kJ/(kg · K). The cycle is closed by a fictitious isobaric process (3H) → (1) of heat rejection to the open ambient conditions. A single value of specific heat ratio $\gamma = 1.242$ appears sufficient for such an analysis but with $R = 348$ kJ/(kg · K) and 396 kJ/(kg · K) for the isochoric compression and for the isentropic expansion respectively.

B. The Fickett–Jacobs Cycle

The FJ cycle, as can be seen in Fig. 1, consists of a compression and heat addition process that brings the gas from state (1) to state (2CJ). This process is strictly a nonequilibrium one. Recall that the CJ theory

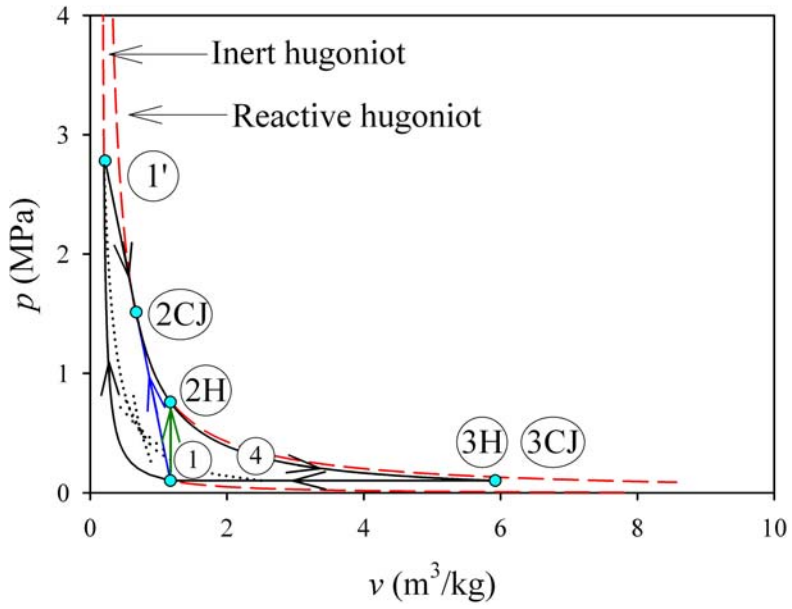

(a) p–v diagram.

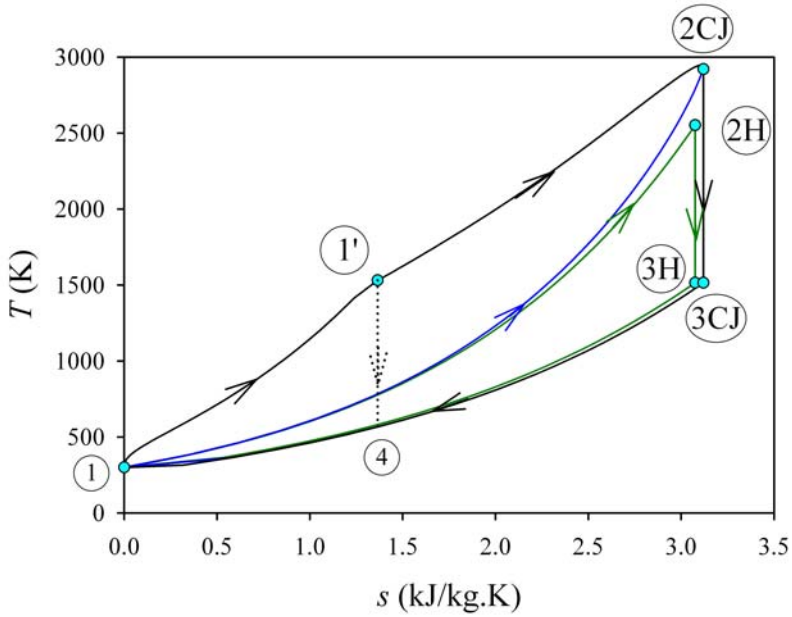

(b) T–s diagram.

Figure 1. Ideal Humphrey ($1 \rightarrow 2\text{H} \rightarrow 3\text{H} \rightarrow 1$)**, FJ** ($1 \rightarrow 2\text{CJ} \rightarrow 3\text{CJ} \rightarrow 1$) **and ZND** ($1 \rightarrow 1' \rightarrow 2\text{CJ} \rightarrow 3\text{CJ} \rightarrow 1$) **cycles for a stoichiometric hydrogen/air mixture initially at STP.**

assumes an instantaneous heat release (unlike the more elaborate ZND theory). Within the one-dimensional model of the detonation process, this process is identical to Rayleigh heating and thus can be regarded to be a process that is in local thermodynamic equilibrium.[23,24] In other words, the tangent from (1) to (2CJ) in the p-v diagram is the same path as that of Rayleigh heating. Isentropic expansion occurs between (2CJ) and (3CJ) after which the cycle is closed by a fictitious isobaric process to the initial state.

Specifically for a hydrogen–air mixture initially at STP, $p_{2CJ} = 1.5$ MPa and decreases the specific volume to $v_{2CJ} = 0.67$ m^3/kg with the same dimensionless heat release $\alpha = 27.28$ as for the Humphrey cycle. The isentropic expansion from (2CJ) to (3CJ) yields $p_{3CJ} = 0.1$ MPa and $v_{3CJ} = 5.92$ m^3/kg respectively. Finally, a fictitious isobaric process returns both pressure and specific volume to the initial state.

While the calculations of (p_{2CJ}, v_{2CJ}) are straightforward, (T_{2CJ}, s_{2CJ}) are more complicated to determine. The value of the gas constant changes from (1′) to (2CJ) as, for example, in computations using Cantera.[22] For simplicity, a linear variation of R between the value at state (1′) and (2CJ) is accurate for modeling the nonequilibrium heat release, which coincided with the equilibrium Rayleigh heat release. The temperature rises from the ZND value of 1545 K to 2920 K and the entropy rises by 3.12 kJ/(kg · K). The gas then expands isentropically from (2CJ) to (3CJ). State (3CJ) is different from state (3H) because the isentropic expansions arise from the different states (2CJ) and (2H) state, respectively. The values of p_{3CJ}, v_{3CJ} and T_{3CJ} are 0.1 MPa, 5.922 m^3/kg and 1562 K respectively.

For cycle analysis, the tangency relationship must be used to evaluate the CJ point exactly, namely,

$$
\begin{aligned}
v_{CJ} = \Big[&\frac{1}{4}(1+\gamma-\gamma^2-3\gamma^3-2\alpha(1-3\gamma-\gamma^2+3\gamma^3)-v_1(-2+4\gamma^2-2\gamma^3+2\alpha(-1+\gamma^2)-(-1+3\gamma^2)v_1))\\
&((-3-\gamma+5\gamma^2+\gamma^3+2\alpha(-1+\gamma^2)+2\alpha(1-3\gamma-\gamma^2+3\gamma^3)-(-1+3\gamma^2)v_1)^2\\
&-4(-3-2\gamma-2\gamma^2-4\gamma^3-4\alpha(-1-\gamma+\gamma^2+\gamma^3)+(2\gamma^2+2\gamma^3)v_1)(-1+\gamma+\gamma^2-\gamma^3\\
&-2\alpha(-1+3\gamma-3\gamma^2+\gamma^3)+v_1(-2\gamma^2+2\gamma^3+2(1-\gamma-\gamma^2+\gamma^3)(\alpha+v_1))))\Big]\\
&/[-3-2\gamma-2\gamma^2-4\gamma^3-4\alpha(-1-\gamma+\gamma^2+\gamma^3)+(2\gamma^2+2\gamma^3)v_1] \qquad (1)
\end{aligned}
$$

(Details in the derivation of Eq. (1) are found in Appendix A.) This is because the CJ point from an equilibrium calculation, say, using CEA is slightly different from that obtained from a nonequilibrium one, say, using Cantera. Thus, for simplicity, a tangent is cast from the inert to the reactive hugoniot whose intersection is the CJ point.

A similar difficulty is encountered in evaluating T_{CJ} due to the variation of the gas constant R from the initial point. It was found that a linear variation of value of R from (1) to (2CJ) is satisfactory to describe this path in the T–s diagram, which is necessary for cycle analysis for the same reason as above. In summary, the properties at (2CJ) are a total pressure of 1.5 MPa, a total specific volume of 0.67 m^3/kg, a total temperature of 2920 K and an increase of entropy to 3.12 kJ/(kg · K). The FJ cycle then allows the gas to expand isentropically to (3CJ). The properties here at a total pressure of 0.1 MPa, a total specific volume of 5.92 m^3/kg, a total temperature of 1515 K.

C. Zel'dovich–von Neumann–Döring Cycle

The two-step process of the ZND model is shown in Fig. 1 by (1) → (1′) → (2CJ) as described previously. There are no ambiguities in determining (1′) for a real mixture. Calculations using Cantera yield total postshock pressure and specific volume as 2.8 MPa and 0.22 m^3/kg respectively. The subsequent CJ value is the same as the FJ cycle reported above. This is followed by the same isentropic expansion as the FJ cycle, followed by a fictitious isobaric process to close the cycle. Moreover, the shock compression to the ZND point raises the temperature to 1531 K with an entropy increase to 1.366 kJ/(kg · K). The heat addition that brings the gas from the ZND to the CJ point raises the temperature to 2920 K with a further increase of entropy to 3.12 kJ/(kg · K). From Cantera, the gas constant at these two points are 397.6 and 348.22 kJ/(kg · K) respectively. The isentropic expansion to 1 atm lowers the gas temperature to 1515 K. Finally, a fictitious isobaric process closes the cycle.

It is now proposed that the work in a ZND cycle is split into a part that is not available and another that is available, these being known as internal and external work respectively. Consider a shock wave as shown in Fig. 2(a). States (1) and (1′) in the figure refer to the same states as in Fig. 1(a). Figure 2(a) shows an isentropic expansion to state (4) which is shown in Fig. 1(a) by a dotted line. Now, for the control volume to remain stationary, a force must be exerted to equal the change in momentum flux from (1) to (4) with $p_4 = p_1$. In other words, thrust work must be done which is equal to the area enclosed by the path (1) $\underset{\text{shock}}{\rightarrow}$ (1′) → (4) → (1) in Fig. 1(a). This is known as internal work which imparts internal energy to sustain the shock and is unavailable for work production.

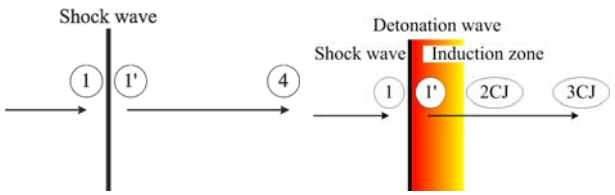

(a) Shock wave followed by isentropic expansion.

(b) Detonation wave followed by isentropic expansion.

Figure 2. The two-step ZND process for a detonation wave.

Turning next to a detonation wave as shown in Fig. 2(b), the process now includes the heat release from (1′) to (2CJ) in the induction zone followed by an isentropic expansion to state (3CJ). The total work available is equal to the area enclosed by the path (1) $\underset{\text{isen}}{\rightarrow}$ (1′) → (2CJ) → (3CJ) → (1). However, based on the above discussion, a certain portion of the work is unavailable. Only the difference in the areas of the two paths in Fig. 1(a) is available, this being known as the external work.

D. Summary

A consideration of the thermodynamics of the Humphrey, FJ and ZND cycles reveals that drastic assumptions are made for all of them to gain some tractability. Of these, it is suggested that the ZND cycle models the actual PDE engine with the proper physics. To summarize, for engineering analysis, we examine the discrepancies in cycle performance due to the three models. The net work out, net heat in and the efficiency are given respectively by

$$w_{out} = \oint P_t \, dv \tag{2a}$$

$$q_{t,in} = \oint T_t \, ds \tag{2b}$$

$$\eta = w_{out}/q_{t,in} \tag{2c}$$

where the subscript t is used to indicate that the total property is being considered. Note that while the same Eq. (2a) is used for the three cycles, the ZND cycle requires that the internal work be neglected. Evaluating the above equations yield results displayed in Table 2. Note that these are cyclic values. A peculiarity of pulse detonation engines is that the cyclic values are likely much larger than the time-averaged values, the latter being dependent on the number of cycles per unit time. When the time required for the fill and purge processes are included, then performance parameters such as *power* or *thrust*, depending on whether the engine is used for power production or for propulsion, will be lower than if the two aforementioned processes are ignored. Nonetheless, this extra complication has no bearing to cycle analysis.

From these results, it can be stated that the ZND cycle accounts for the internal energy in the shock wave while the Humphrey and FJ cycles only account for heat addition. The results point out that the performance parameters are largely underestimated in Humphrey and FJ cycles, which may have a drastic effect on performance analysis.

III. Precompression

As a general statement, all heat engines using compressible substances as the working medium require that the substance be compressed before heat addition. Shock compression by itself may be sufficient to initiate and perhaps sustain cyclic operation although no such practical devices are known to exist. Instead, it is suggested here that sustained cyclic operation requires precompression. For a detonation engine, this precompression need not be large, unlike conventional engines, so that the overall compression does not exceed structural and material limits. The effect of a small amount of precompression is considered, with compressor pressure ratios $\pi_c = 1$–3 for a hydrogen–air mixture initially at STP.

The results are shown in Fig. 3 and Table 3. The cycle work remains fairly constant but the heat input increases with increasing compression. The results show that the cycle efficiency decreases slightly with increasing compression.

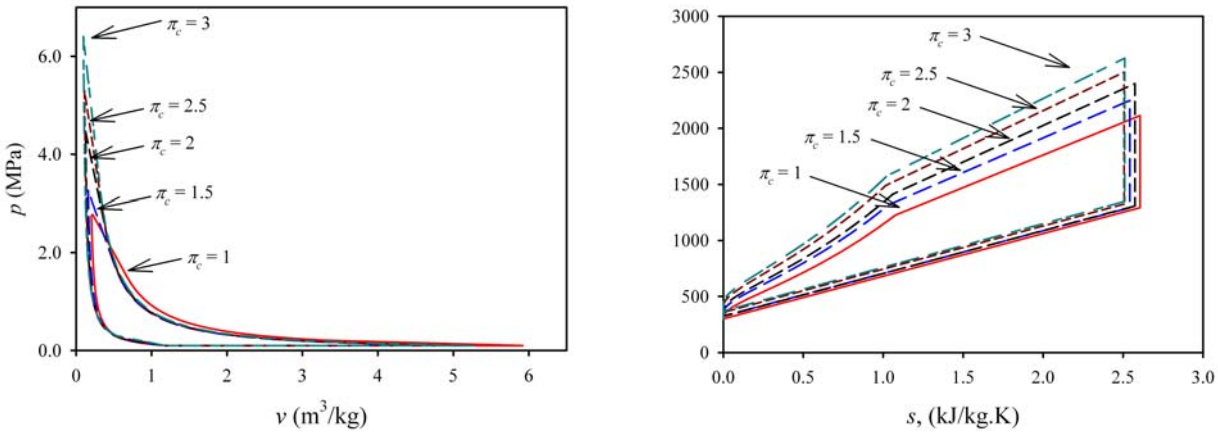

(a) p–v diagram.

(b) T–s diagram.

Figure 3. ZND cycle with precompression. Isentropes not shown for clarity.

IV. Arbitrary Heat Release

Finally, instead of a specific reactant mixture, an arbitrary heat release is considered here. The nondimensional heat release α ranges from 10 to 30, which covers most reactant mixtures of interest for PDEs. Figure 4 shows the ZND cycles for this range of α with a precompression ratio $\pi_c = 3$. The work out and

Table 2. Performance comparisons of the three cycles.

	Humphrey	Fickett–Jacobs	Zel'dovich–von Neumann–Döring
Work out (MJ/kg)	0.709	0.834	1.40
Heat in (MJ/kg)	1.07	1.3	2.29
Efficiency (%)	66.5	64.3	61.2

heat in per cycle and the cyclic efficiency are listed in Table 4. Not surprisingly, the more energetic fuel yields a higher cycle efficiency.

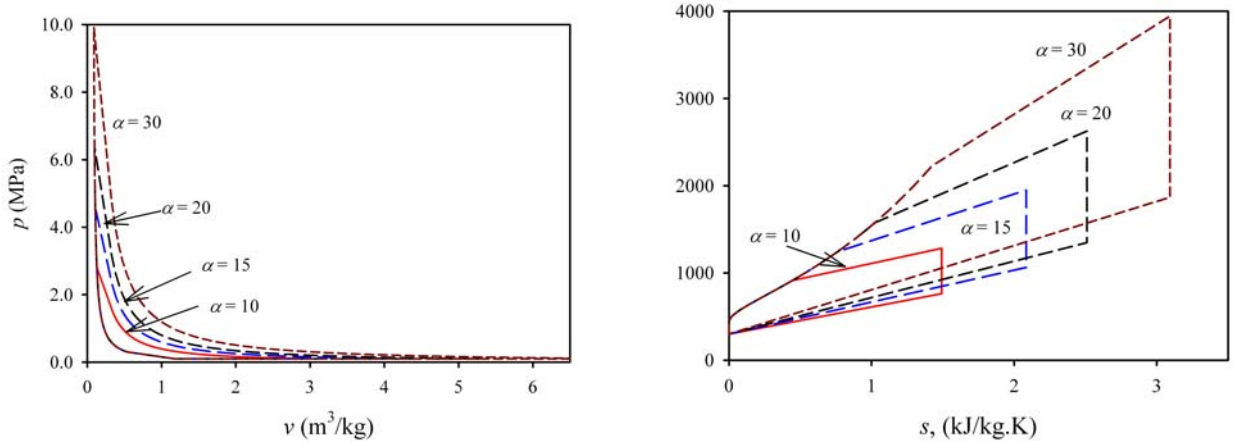

(a) p–v diagram.

(b) T–s diagram.

Figure 4. ZND cycle with arbitrary heat release with $\pi_c = 3$. Isentropes not shown for clarity.

Table 3. Performance of ZND cycle for stoichiometric hydrogen–air mixture initially at STP with precompression.

$\pi_c =$	1	1.5	2	2.5	3
Work out (MJ/kg)	1.40	1.45	1.45	1.45	1.42
Heat in (MJ/kg)	2.29	2.49	2.62	2.70	2.76
Efficiency (%)	61.2	58.5	55.6	53.7	51.5

V. Conclusion

An appraisal three thermodynamic cycles for modeling pulse detonation engines was performed. The Zel'dovich–von Neumann–Döring cycle was deemed to be the most appropriate. This requires an assumption of local thermodynamic equilibrium in the shock process. It was found that the heat addition process can be modeled by a supersonic Rayleigh heating process. Additionally, it was suggested that the shock causes a certain amount of work to be unavailable. The analysis was performed using a stoichiometric hydrogen–air mixture initially at STP. Inclusion of precompression revealed that the efficiency decreases with compressor pressure ratio. A generic heat addition process was also considered. In this case, it was found that an energetic material with higher heat release yields an increased thermodynamic efficiency.

References

[1]Bejan, A., *Advanced Engineering Thermodynamics*, Wiley, Hoboken, New Jersey, 3rd ed., 2006.

[2]Humphrey, H. A., "An Internal-Combustion Pump, and Other Applications of a New Principle," *Proceedings of the Institution of Mechanical Engineers*, Vol. 77, No. 1, 1909, pp. 1075–1200.

[3]Chapman, D. L., "On the Rate of Explosion in Gases," *Philosophical Magazine Series 5*, Vol. 47, No. 284, 1889, pp. 90–104.

[4]Jouguet, E., "Sur la propagation des réactions chimiques dans les gaz," *Journal des Mathématiques Pures et Appliquées*, Vol. 1 and 2, 1905 and 1906, pp. 347–425 and 5–86, (On the Propagation of Chemical Reactions in Gases).

[5]Kuo, K. K., *Principles of Combustion*, Wiley, New York, 2nd ed., 2005.

[6]Lee, J. H. S., *The Detonation Phenomenon*, Cambridge, New York, 2008.

[7]Zeldovich, Y. B., "K Teori rasprostranenia detonazi v gasoobrasnikh systemakh," *Zhurnal Experimental'noi i Teoreticheskoi Fiziki*, Vol. 10, 1940, pp. 543–568, English translation: On the Theory of the Propagation of Detonation in Gaseous Systems, NACA TM 1261, 1960.

[8]von Neumann, J., "Theory of Detonation Waves. Progress Report to the National Defense Research Committee Div. B, OSRD-549, (April 1, 1942. PB 31090)," *John von Neumann: Collected Works, 1903–1957*, edited by A. H. Taub, Vol. 6, Pergamon, New York, 1963.

[9]Döring, W., "Über den Detonationsvorgang in Gasen," *Annalen der Physik*, Vol. 43, 1943, pp. 421–436, (On the Detonation Process in Gases); volume renumbered to vol. 435, no. 6.

[10]Heiser, W. H. and Pratt, D. T., "Thermodynamic Cycle Analysis of Pulse Detonation Engine," *Journal of Propulsion and Power*, Vol. 18, No. 1, 2002, pp. 68–76.

[11]Kentfield, J. A. C., "Thermodynamic Cycle Analysis of Pulse Detonation Engine," *Journal of Propulsion and Power*, Vol. 18, No. 1, 2002, pp. 68–76, doi: 10.2514/2.5899.

[12]Talley, D. G. and Coy, E. B., "Constant Volume Limit of Pulsed Propulsion for a Constant γ Ideal Gas," *Journal of Propulsion and Power*, Vol. 18, No. 2, 2002, pp. 400–406, doi: 10.2514/2.5948.

[13]Hutchins, T. E. and Metghalchi, M., "Energy and Exergy Analyses of the Pulse Detonation Engine," *Journal of Engineering for Gas Turbines and Power*, Vol. 125, No. 4, 2003, pp. 1075–1080.

[14]Wu, Y., Ma, F., and Yang, V., "System Performance and Thermodynamic Cycle Analysis of Airbreathing Pulse-Detonation Engines," *Journal of Propulsion and Power*, Vol. 19, No. 4, 2003, pp. 556–567.

[15]Bellini, R. and Lu, F. K., "Exergy analysis of a pulse detonation power device," *Journal of Propulsion and Power*, Vol. 26, No. 4, 2010, pp. 875–878.

[16]Li, J. L., Fan, W., Wang, Y.-Q., Qui, H., and Yan, C.-J., "Performance Analysis of the Pulse Detonation Rocket Engine Based on Constant Volume Cycle Model," *Applied Thermal Engineering*, Vol. 30, No. 11–12, 2010, pp. 1496–1504.

[17]Braun, E. M., Lu, F. K., Wilson, D. R., and Camberos, J., "Detonation Engine Performance Comparison Using First and Second Law Analyses," AIAA Paper 2010–7040, 2010.

[18]Wintenberger, E. and Shepherd, J. E., "Thermodynamic Cycle Analysis for Propagating Detonations," *Journal of Propulsion and Power*, Vol. 22, No. 3, 2006, pp. 694–698.

[19]Vilar, J. M. G. and Rub, J. M., "Thermodynamics "Beyond" Local Equilibrium," *Proceedings of the National Academy of Sciences*, Vol. 98, No. 20, 2001, pp. 11081–11084.

[20]Casas-Vázquez, J. and Jou, D., "Temperature in Non-Equilibrium States: A Review of Open Problems and Current Proposals," *Reports on Progress in Physics*, Vol. 66, No. 11, 2003, pp. 1937–2023.

[21]Gordon, S. and McBride, B. J., "Computer Program for Calculation of Complex Chemical Equilibrium Compositions and Applications, I: Analysis," NASA RP 1311, 1994.

[22]Goodwin, D., "Cantera: Object-Oriented Software for Reacting Flows," http://code.google.com/p/cantera, 2010.

[23]Liu, Z. Y., *Overdriven Detonation Phenomenon and Its Application to Ultra-High Pressure Generation*, Ph.D. thesis, Kumamoto University, 2001.

[24]Rao, S., *Effect of Friction on the Zel'dovich–von Neumann–Döoring to Chapman–Jouguet Transition*, Master's thesis, University of Texas at Arlington, 2010.

Table 4. Performance of ZND cycle for different arbitrary values of nondimensional heat release of a reactive mixture initially at STP.

$\alpha =$	10	15	20	30
Work out (MJ/kg)	0.521	1.06	1.42	2.81
Heat in (MJ/kg)	1.03	1.97	2.76	5.02
Efficiency (%)	50.5	53.7	51.5	56.0

A. The Rankine–Hugoniot Relationship and the Upper CJ Point

Other than available software such as CEA and Stanjan, the CJ state can also be obtained analytically. The hugoniot in general is given by

$$\frac{p_2}{p_1} = \frac{(\gamma+1) - (\gamma-1)\frac{v_1}{v_2} + (2(\gamma-1)\alpha)}{(\gamma+1)\frac{v_1}{v_2} - (\gamma-1)} \tag{3}$$

where $\alpha = q\rho_1/p_1$ is the nondimensional heat release parameter. By definition, the CJ point is located by the tangent from the initial state to the reactive Hugoniot. The slope of the tangent is given by

$$m = \frac{(1-\gamma^2)[(\gamma+1) - (\gamma-1)v_1 + 2(\gamma-1)\alpha]}{(\gamma+1)v_{CJ} - (\gamma+1)} \tag{4}$$

Now,

$$m = \frac{p_{CJ} - p_1}{v_{CJ} - v_1} \tag{5}$$

Manipulating Eqs. (3)–(5) yields Eq. (1).